

<sup>1</sup> The human visual system preserves the hierarchy  
<sup>2</sup> of 2-dimensional pattern regularity

<sup>3</sup> Peter J. Kohler<sup>1,2,3</sup> and Alasdair D. F. Clarke<sup>4</sup>

<sup>4</sup> *<sup>1</sup> York University, Department of Psychology, Toronto, ON M3J 1P3, Canada*

<sup>5</sup> *<sup>2</sup> Centre for Vision Research, York University, Toronto, ON, M3J 1P3, Canada*

<sup>6</sup> *<sup>3</sup>Stanford University, Department of Psychology, Stanford, CA 94305, United States*

<sup>7</sup> *<sup>4</sup>University of Essex, Department of Psychology, Colchester, UK, CO4 3SQ*

<sup>8</sup> **Abstract**

Symmetries are present at many scales in images of natural scenes. A large body of literature has demonstrated contributions of symmetry to numerous domains of visual perception. The four fundamental symmetries, reflection, rotation, translation and glide reflection, can be combined in exactly 17 distinct ways. These *wallpaper groups* represent the complete set of symmetries in 2D images and have recently found use in the vision science community as an ideal stimulus set for studying the perception of symmetries in textures. The goal of the current study is to provide a more comprehensive description of responses to symmetry in the human visual system, by collecting both brain imaging (Steady-State Visual Evoked Potentials measured using high-density EEG) and behavioral (symmetry detection thresholds) data using the entire set of wallpaper groups. This allows us to probe the hierarchy of complexity among wallpaper groups, in which simpler groups are subgroups of more complex ones. We find that this hierarchy is preserved almost perfectly in both behavior and brain activity: A multi-level Bayesian GLM indicates that for most of the 63 subgroup relationships, subgroups produce lower amplitude responses in visual cortex (posterior probability: > 0.95 for 56 of 63) and require longer presentation durations to be reliably detected (posterior probability: > 0.95 for 49 of 63). This systematic pattern is seen only in visual cortex and only in components of the brain response known to be symmetric-specific. Our results show that representations of symmetries in the human brain are precise and rich in detail, and that this precision is reflected in behavior. These findings expand our understanding of symmetry perception, and open up new avenues for research on how fine-grained representations of regular textures contribute to natural vision.

Symmetries are abundant in natural and man-made environments, due to a complex interplay of physical forces that govern pattern formation in nature. Symmetrical patterns have been created and appreciated by human cultures throughout history and since the gestalt movement of the early 20th century, symmetry has been recognized as important for visual perception. Symmetry contributes to the perception of shapes (Palmer, 1985; Li et al., 2013), scenes (Apthorp and Bell, 2015) and surface properties (Cohen and Zaidi, 2013), as well as the social process of mate selection (Møller, 1992). Most of this work has focused on mirror symmetry or *reflection*, with much less attention being paid to the other fundamental symmetries: *rotation*, *translation*

38 and *glide reflection*. In the two spatial dimensions relevant for images, these four symmetries can  
39 be combined in 17 distinct ways, *the wallpaper groups* (Fedorov, 1891; Polya, 1924; Liu et al., 2010).  
40 Previous work on a subset of four of the wallpaper groups used functional MRI to demonstrate  
41 that rotation symmetries in wallpapers elicit parametric responses in several areas in occipital  
42 cortex, beginning with visual area V3 (Kohler et al., 2016). This effect was also robust with  
43 electroencephalography (EEG), whether measured using Steady-State Visual Evoked Potentials  
44 (SSVEPs) (Kohler et al., 2016) or event-related paradigms (Kohler et al., 2018). Here we extend this  
45 work by collecting SSVEPs and psychophysical data from human participants viewing the full set  
46 of wallpaper groups. We measure responses in visual cortex to 16 out of the 17 wallpaper groups,  
47 with the 17th serving as a control stimulus. Our goal is to provide a more complete picture of  
48 how wallpaper groups are represented in the human visual system.

49 A wallpaper group is a topologically discrete group of isometries of the Euclidean plane, i.e.  
50 transformations that preserve distance (Liu et al., 2010). Wallpaper groups differ in the number  
51 and kind of these transformations. In mathematical group theory, when the elements of one  
52 group is completely contained in another, the inner group is called a subgroup of the outer  
53 group (Liu et al., 2010). The full list of subgroup relationships is listed in Section 1.4.2 of the  
54 Supplementary Material. Subgroup relationships between wallpaper groups can be distinguished  
55 by their indices. The index of a subgroup relationship is the number of cosets, i.e. the number  
56 of times the subgroup is found in the supergroup (Liu et al., 2010). As an example, let us consider  
57 groups  $P_2$  and  $P_6$ . If we ignore the translations in two directions that both groups share, group  $P_6$   
58 consists of the set of rotations  $\{0^\circ, 60^\circ, 120^\circ, 180^\circ, 240^\circ, 300^\circ\}$ , in which  $P_2 \{0^\circ, 180^\circ\}$  is contained.  
59  $P_2$  is thus a subgroup of  $P_6$ , and  $P_6$  can be generated by combining  $P_2$  with rotations  $\{0^\circ, 120^\circ,$   
60  $240^\circ\}$ . Because  $P_2$  is repeated three times in  $P_6$ ,  $P_2$  is a subgroup of  $P_6$  with index 3 (Liu et al.,  
61 2010). The 17 wallpaper groups thus obey a hierarchy of complexity where simpler groups are  
62 subgroups of more complex ones (Coxeter and Moser, 1972).

63 The two datasets we present here make it possible to assess the extent to which both behavior  
64 and brain responses follow the hierarchy of complexity expressed by the subgroup relationships.  
65 Based on previous brain imaging work showing that patterns with more axes of symmetry pro-  
66 duce greater activity in visual cortex (Sasaki et al., 2005; Kohler et al., 2018, 2016; Keefe et al., 2018),  
67 we hypothesized that more complex groups would produce larger SSVEPs. For the psychophys-  
68 ical data, we hypothesized that more complex groups would lead to shorter symmetry detection  
69 thresholds, based on previous data showing that under a fixed presentation time, discriminability  
70 increases with the number of symmetry axes in the pattern (Wagemans et al., 1991). Our results  
71 confirm both hypotheses, and show that activity in human visual cortex is remarkably consistent  
72 with the hierarchical relationships between the wallpaper groups, with SSVEP amplitudes and  
73 psychophysical thresholds following these relationships at a level that is far beyond chance. The  
74 human visual system thus appears to encode all of the fundamental symmetries using a represen-  
75 tational structure that closely approximates the subgroup relationships from group theory.

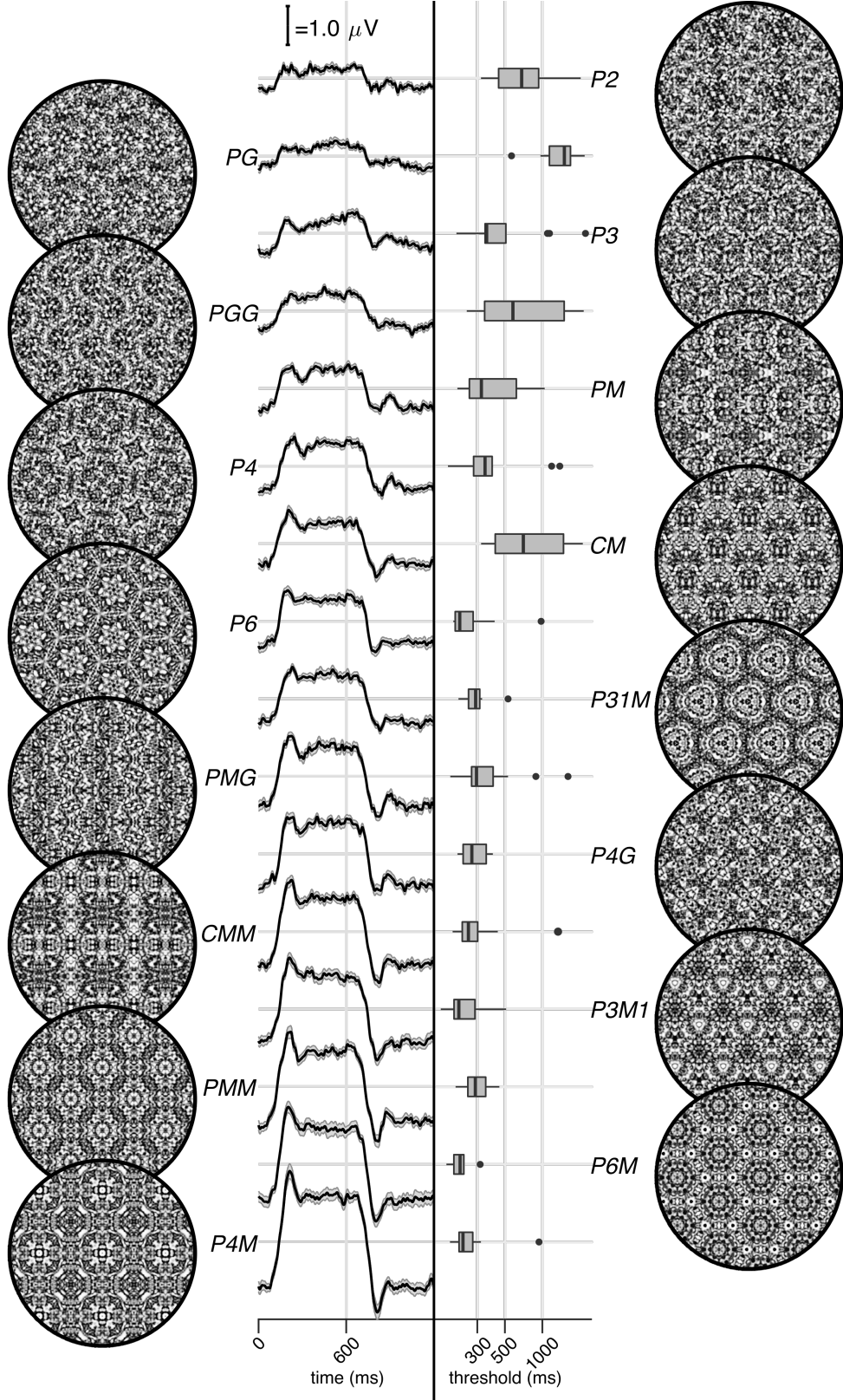


Figure 1: Examples of each of the 16 wallpaper groups are shown in the left- and right-most column of the figures, next to the corresponding SSVEP (center-left) and psychological (center-right) data from each group. The SSVEP data are odd-harmonic-filtered cycle-average waveforms. In each cycle, a  $P_1$  exemplar was shown for the first 600 ms, followed by the original exemplar for the last 600 ms. Errorbars are standard error of the mean. Psychophysical data are presented as boxplots reflecting the distribution of display duration thresholds. The 16 groups are ordered by the strength of the SSVEP response, to highlight the range of response amplitudes.

76 **Results**

77 The stimuli used in our two experiments were generated from random-noise textures, which  
78 made it possible to generate multiple exemplars from each of the wallpaper groups, as described  
79 in detail elsewhere (Kohler et al., 2016). We generated control stimuli matched to each exemplar  
80 in the main stimulus set, by scrambling the phase but maintaining the power spectrum. All  
81 wallpaper groups are inherently periodic because of their repeating lattice structure. Phase  
82 scrambling maintains this periodicity, so the phase-scrambled control images all belong to group  
83  $P_1$  regardless of group membership of the original exemplar.  $P_1$  contains no symmetries other  
84 than translation, while all other groups contain translation in combination with one or more of the  
85 other three fundamental symmetries (reflection, rotation, glide reflection) (Liu et al., 2010). In our  
86 SSVEP experiment, this stimulus set allowed us to isolate brain activity specific to the symmetry  
87 structure in the exemplar images from activity associated with modulation of low-level features,  
88 by alternating exemplar images and control exemplars. In this design, responses to structural  
89 features beyond the shared power spectrum, including any symmetries other than translation,  
90 are isolated in the odd harmonics of the image update frequency (Kohler et al., 2016; Norcia et al.,  
91 2015, 2002). Thus, the combined magnitude of the odd harmonic response components can be  
92 used as a measure of the overall strength of the visual cortex response.

93 The psychophysical experiment took a distinct but related approach. In each trial an exemplar  
94 image was shown with its matched control, one image after the other, and the order varied pseudo-  
95 randomly such that in half the trials the original exemplar was shown first, and in the other half  
96 the control image was shown first. After each trial, participants were instructed to indicate  
97 whether the first or second image contained more structure. The duration of both images was  
98 controlled by a staircase procedure so that a threshold duration for symmetry detection could be  
99 computed for each wallpaper group.

100 Examples of the wallpaper groups and a summary of our brain imaging and psychophysical  
101 measurements are shown in Figure 1. For our primary SSVEP analysis, we only considered EEG  
102 data from a pre-determined region-of-interest (ROI) consisting of six electrodes over occipital cor-  
103 tex (see Supplementary Figure 1.1). SSVEP data from this ROI was filtered so that only the odd  
104 harmonics that capture the symmetry response contribute to the waveforms. While waveform am-  
105 plitude is quite variable among the 16 groups, all groups have a sustained negative-going response  
106 that begins at about the same time for all groups, 180 ms after the transition from the  $P_1$  control  
107 exemplar to the original exemplar. To reduce the amplitude of the symmetry-specific response to  
108 a single number that could be used in further analyses and compared to the psychophysical data,  
109 we computed the root-mean-square (RMS) over the odd-harmonic-filtered waveforms. The data  
110 in Figure 1 are shown in descending order according to RMS. The psychophysical results, shown  
111 in box plots in Figure 1, were also quite variable between groups, and there seems to be a general  
112 pattern where wallpaper groups near the top of the figure, that have lower SSVEP amplitudes,  
113 also have longer psychophysical threshold durations.

114 We now wanted to test our two hypotheses about how SSVEP amplitudes and threshold du-  
115 rations would follow subgroup relationships, and thereby quantify the degree to which our two  
116 measurements were consistent with the group theoretical hierarchy of complexity. We tested

each hypothesis using the same approach. We first fitted a Bayesian model with wallpaper group as a factor and participant as a random effect. We fit the model separately for SSVEP RMS and psychophysical data and then computed posterior distributions for the difference between supergroup and subgroup. These difference distributions allowed us to compute the conditional probability that the supergroup would produce (a) larger RMS and (b) a shorter threshold durations, when compared to the subgroup. The posterior distributions are shown in Figure 2 for the SSVEP data, and in Figure 3 for the psychophysical data, which distributions color-coded according to conditional probability. For both data sets our hypothesis is confirmed: For the overwhelming majority of the 63 subgroup relationships, supergroups are more likely to produce larger symmetry-specific SSVEPs and shorter symmetry detection threshold durations, and in most cases the conditional probability of this happening is extremely high.

We also ran a control analysis using (1) odd-harmonic SSVEP data from a six-electrode ROI over parietal cortex (see Supplementary Figure 1.1) and (2) even-harmonic SSVEP data from the same occipital ROI that was used in our primary analysis. By comparing these two control analysis to our primary SSVEP analysis, we can address the specify of our effects in terms of location (occipital cortex vs parietal cortex) and harmonic (odd vs even). For both control analyses (plotted in Supplementary Figures 3.3 and 3.4), the correspondence between data and subgroup relationships was substantially weaker than in the primary analysis. We can quantify the strength of the association between the data and the subgroup relationships, by asking what proportion of subgroup relationships that reach or exceed a range of probability thresholds. This is plotted in Figure 4, for our psychophysical data, our primary SSVEP analysis and our two control SSVEP analyses. It shows that odd-harmonic SSVEP data from the occipital ROI and symmetry detection threshold durations both have a strong association with the subgroup relationships such that a clear majority of the subgroups survive even at the highest threshold we consider ( $p(\Delta > 0 | data) > 0.99$ ). The association is far weaker for the two control analyses.

SSVEP data from four of the wallpaper groups ( $P_2, P_3, P_4$  and  $P_6$ ) was previously published as part of our earlier demonstration of parametric responses to rotation symmetry in wallpaper groups (Kohler et al., 2016). We replicate that result using our Bayesian approach, and find an analogous parametric effect in the psychophysical data (see Supplementary Figure 4.1). We also conducted an analysis testing for an effect of index in our two datasets and found that subgroup relationships with higher indices tended to produce greater pairwise differences between the subgroup and supergroup, for both SSVEP RMS and symmetry detection thresholds (see Supplementary Figure 4.2). The effect of index is relatively weak, but the fact that there is a measurable index effect can nonetheless be taken as preliminary evidence that representations of symmetries in wallpaper groups may be compositional.

Finally, we conducted a correlation analysis comparing SSVEP and psychophysical data and found a reliable correlation ( $R^2 = 0.44$ , Bayesian confidence interval [0.28, 0.55]). The correlation reflects an inverse relationship: For subgroup relationships where the supergroup produces a much *larger* SSVEP amplitude than the subgroup, the supergroup also tends to produce a much *smaller* symmetry detection threshold. This is consistent with our hypotheses about how the two measurements relate to symmetry representations in the brain, and suggests that our brain

158 imaging and psychophysical measurements are at least to some extent tapping into the same  
159 underlying mechanisms.

160 **Discussion**

161 Here we show that beyond merely responding to the elementary symmetry operations of reflection  
162 (Sasaki et al., 2005) and rotation (Kohler et al., 2016), the visual system represents the hierarchi-  
163 cal structure of the 17 wallpaper groups, and thus every composition of the four fundamental  
164 symmetries (rotation, reflection, translation, glide reflection) which comprise the set of regular  
165 textures. Both SSVEP amplitudes and symmetry detection thresholds preserve the hierarchy of  
166 complexity among the wallpaper groups that is captured by the subgroup relationships (Coxeter  
167 and Moser, 1972). For the SSVEP, this remarkable consistency was specific to the odd harmonics of  
168 the stimulus frequency that are known to capture the symmetry-specific response (Kohler et al.,  
169 2016) and to electrodes in a region-of-interest (ROI) over occipital cortex. When the same analysis  
170 was done using the odd harmonics from electrodes over parietal cortex (Supplementary Figure  
171 3.3) or even harmonics from electrodes over occipital cortex (Supplementary Figure 3.4), the data  
172 was substantially less consistent with the subgroup relationships (yellow and green lines, Figure  
173 4).

174 The current data provide a description of the visual system's response to the complete set of  
175 symmetries in the two-dimensional plane. Our design precludes us from independently measure  
176 the response to  $P_1$ , but because each of the 16 other groups produce non-zero odd harmonic  
177 amplitudes (see Figure 1), we can conclude that the relationships between  $P_1$  and all other groups,  
178 where  $P_1$  is the subgroup, are also preserved by the visual system. The subgroup relationships  
179 are in many cases not obvious perceptually, and most participants had no knowledge of group  
180 theory. Thus, the visual system's ability to preserve the subgroup hierarchy does not depend  
181 on explicit knowledge of the relationships. Previous behavioral experiments have shown that  
182 although naïve observers can distinguish many of the wallpaper groups (Landwehr, 2009), they  
183 tend to sort them into fewer groups than there actually are (4-12 groups) and it is common for  
184 exemplars from different wallpaper groups to be sorted in the same group (Clarke et al., 2011). The  
185 more controlled two-interval forced choice approach used in the current behavioral experiment  
186 allows us to show that more granular representations of wallpaper groups are measurable in  
187 behavior.

188 We observe a reliable correlation between our brain imaging and psychophysical data. This  
189 suggests that the two measurements reflect the same underlying symmetry representations in  
190 visual cortex. While it should be noted that the correlation is relatively modest ( $R^2 = 0.44$ ), we  
191 note that this may be partly due to the fact that the same individuals did not participate in the  
192 two experiments. Future work in which behavioral and brain imaging data are collected from the  
193 same participants, will help further establish the connection between the two measurements, and  
194 tease apart any additional complexity that may not have been captured by the summary statistics  
195 we applied here. It has recently been demonstrated that  $W$ , a measure of perceptual goodness  
196 derived from a holographic model of regularity (van der Helm and Leeuwenberg, 1996), can

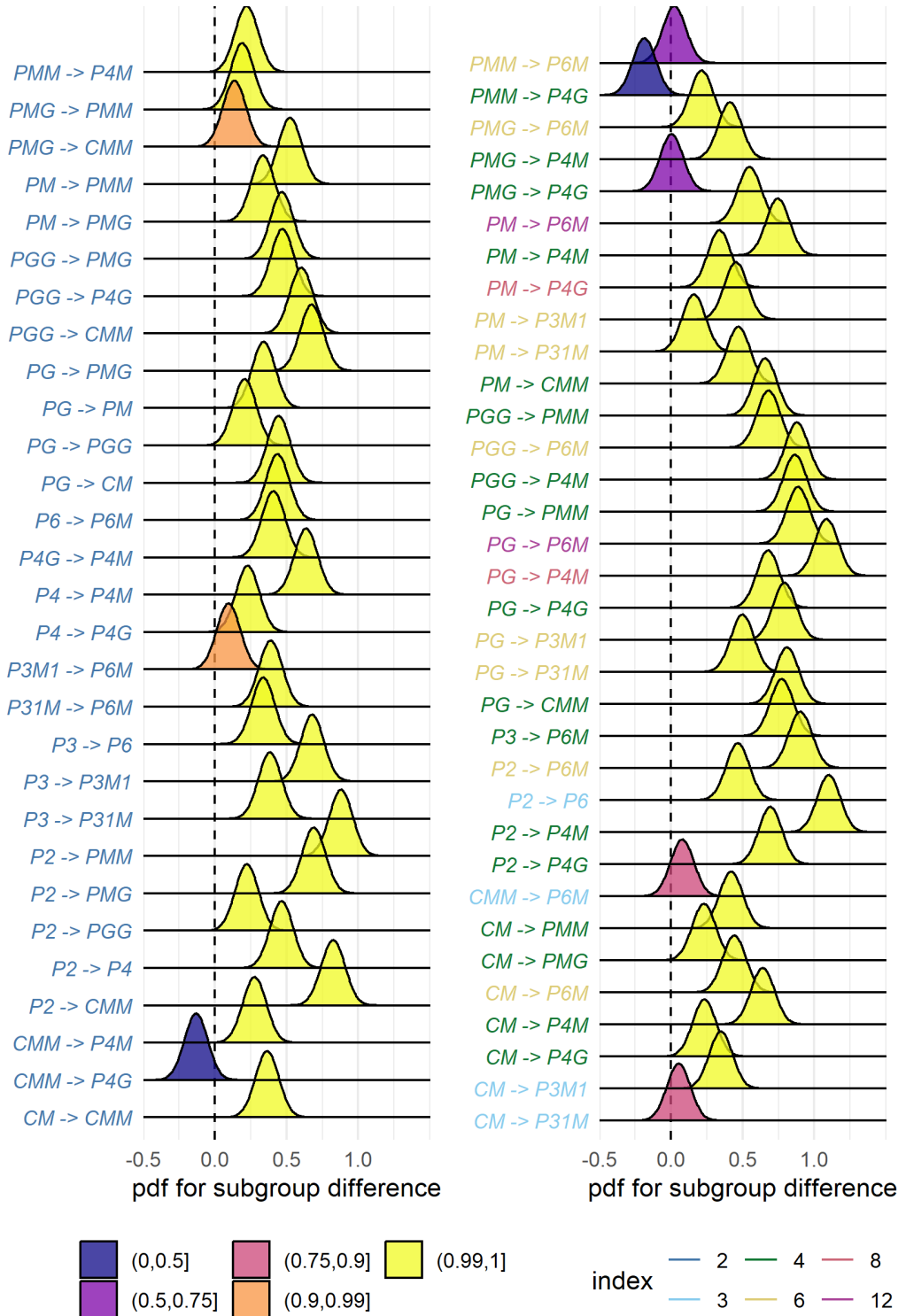


Figure 2: Posterior distributions for the difference in mean SSVEP RMS amplitude. Colour coding of the text indicates the index of the subgroup, while the colour of the filled distribution relates to the conditional probability that the difference in means is greater than zero. We can see that 55/63 subgroup relationships have  $p(\Delta|data) > 0.99$ .

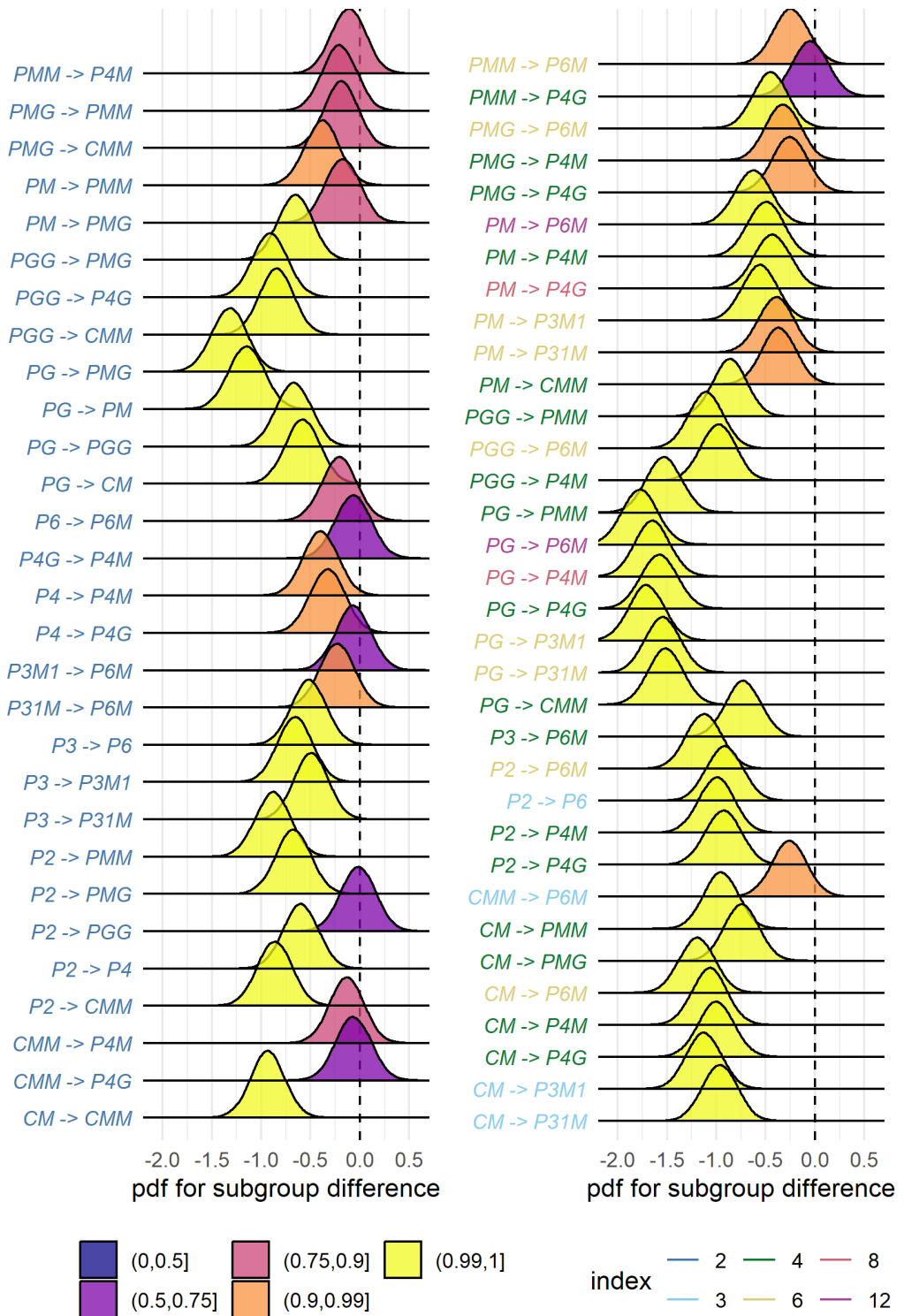


Figure 3: Posterior distributions for the difference in mean symmetry detection threshold durations. Colour coding of the text indicates the index of the subgroup, while the colour of the filled distribution relates to the conditional probability that the difference in means is greater than zero. We can see that 43/63 subgroup relationships have  $p(\Delta|data) > 0.99$ .

predict EEG responses (Makin et al., 2016) and perceptual discrimination performance (Nucci and Wagemans, 2007) for patterns that contain symmetry and other types of regularity. The model was formulated based on dot patterns with symmetry axes centered on a single spatial location. It will be important to determine if and how  $W$  can be computed for our random-noise based wallpaper textures where combinations of symmetries tile the plane, and test how well it can explain behavioral and brain responses to wallpapers.

We also find an effect of index for both our brain imaging measurements and our symmetry detection thresholds. This means that the visual system not only represents the hierarchical relationship captured by individual subgroups, but also distinguishes between subgroups depending on how many times the subgroup is repeated in the supergroup, with more repetitions leading to larger pairwise differences. Our measured effect of index is relatively weak. This is perhaps because the index analysis does not take into account the *type* of isometries that differentiate the subgroup and supergroup. The effect of symmetry type can be observed by contrasting the measured SSVEP amplitudes and detection thresholds for groups *PM* and *PG* in Figure 1. The two groups are comparable except *PM* contains reflection and *PG* contains glide reflection, and the former clearly elicits higher amplitudes and lower thresholds. An important goal for future work will be to map out how different symmetry types contribute to the representational hierarchy.

The correspondence between responses in the visual system and group theory that we demonstrate here, may reflect a form of implicit learning that depends on the structure of the natural world. The environment is itself constrained by physical forces underlying pattern formation and these forces are subject to multiple symmetry constraints (Hoyle, 2006). The ordered structure of responses to wallpaper groups could be driven by a central tenet of neural coding, that of efficiency. If coding is to be efficient, neural resources should be distributed to capture the structure of the environment with minimum redundancy considering the visual geometric optics, the capabilities of the subsequent neural coding stages and the behavioral goals of the organism (Attneave, 1954; Barlow, 1961; Laughlin, 1981; Geisler et al., 2009). Early work within the efficient coding framework suggested that natural images had a  $1/f$  spectrum and that the corresponding redundancy between pixels in natural images could be coded efficiently with a sparse set of oriented filter responses, such as those present in the early visual pathway (Field, 1987; Olshausen and Field, 1997). Our results suggest that the principle of efficient coding extends to a much higher level of structural redundancy – that of symmetries in visual images.

The 17 wallpaper groups are completely regular, and relatively rare in the visual environment, especially when considering distortions due to perspective and occlusion. Near-regular textures, however, abound in the visual world, and can be approximated as deformed versions of the wallpaper groups (Liu et al., 2004). The correspondence between visual cortex responses and group theory demonstrated here may indicate that the visual system represents visual textures using a similar scheme, with the wallpaper groups serving as anchor points in representational space. This framework resembles norm-based encoding strategies that have been proposed for other stimulus classes, most notably faces (Leopold et al., 2006), and leads to the prediction that adaptation to wallpaper patterns should distort perception of near-regular textures, similar to the aftereffects found for faces (Webster and MacLin, 1999). Field biologists have demonstrated

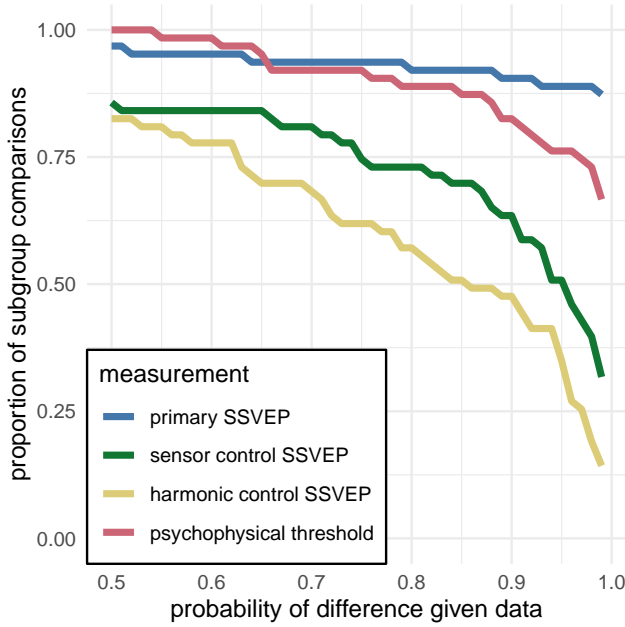


Figure 4: This plot shows the proportion of subgroup relationships that satisfy  $p(\Delta > 0 | data) > x$ . We can see that if we take  $x = 0.95$  as our threshold, the subgroup relationships are preserved in  $56/63 = 89\%$  and  $49/64 = 78\%$  of the comparisons for the primary SSVEP and threshold duration datasets, respectively. This compares to the  $32/64 = 50\%$  and  $22/64 = 35\%$  for the SSVEP control datasets.

that animals respond more strongly to exaggerated versions of a learned stimulus, referred to as “supernormal” stimuli (Tinbergen, 1953). In the norm-based encoding framework, wallpaper groups can be considered *supertextures*, exaggerated examples of the near-regular textures that surround us. Artists may consciously or unconsciously create supernormal stimuli, to capture the essence of the subject and evoke strong responses in the audience (Ramachandran and Hirstein, 1999). Wallpaper groups are visually compelling, and symmetries have been widely used in human artistic expression going back to the Neolithic age (Jablan, 2014). If wallpapers are in fact supertextures, this prevalence may be a direct result of the strategy the human visual system has adopted for texture encoding.

## Participants

Twenty-five participants (11 females, mean age  $28.7 \pm 13.3$ ) took part in the EEG experiment. Their informed consent was obtained before the experiment under a protocol that was approved by the Institutional Review Board of Stanford University. 11 participants (8 females, mean age  $20.73 \pm 1.21$ ) took part in the psychophysics experiment. All participants had normal or corrected-to-normal vision. Their informed consent was obtained before the experiment under a protocol that was approved by the University of Essex’s Ethics Committee.

254 **Stimulus Generation**

255 Exemplars from the different wallpaper groups were generated using a modified version of the  
256 methodology developed by Clarke and colleagues(Clarke et al., 2011) that we have described in de-  
257 tail elsewhere(Kohler et al., 2016). Briefly, exemplar patterns for each group were generated from  
258 random-noise textures, which were then repeated and transformed to cover the plane, according  
259 to the symmetry axes and geometric lattice specific to each group. The use of noise textures as  
260 the starting point for stimulus generation allowed the creation of an almost infinite number of  
261 distinct exemplars of each wallpaper group. To make individual exemplars as similar as possible  
262 we replaced the power spectrum of each exemplar with the median across exemplars within a  
263 group. We then generated control exemplars that had the same power spectrum as the exemplar  
264 images by randomizing the phase of each exemplar image. The phase scrambling eliminates ro-  
265 tation, reflection and glide-reflection symmetries within each exemplar, but the phase-scrambled  
266 images inherent the spectral periodicity arising from the periodic tiling. This means that all  
267 control exemplars, regardless of which wallpaper group they are derived from, are transformed  
268 into another symmetry group, namely  $P_1$ .  $P_1$  is the simplest of the wallpaper groups and contains  
269 only translations of a region whose shape derives from the lattice. Because the different wallpaper  
270 groups have different lattices,  $P_1$  controls matched to different groups have different power spectra.  
271 Our experimental design takes these differences into account by comparing the neural responses  
272 evoked by each wallpaper group to responses evoked by the matched control exemplars.

273 **Stimulus Presentation**

274 Stimulus Presentation. For the EEG experiment, the stimuli were shown on a 24.5" Sony Trimas-  
275 ter EL PVM-2541 organic light emitting diode (OLED) display at a screen resolution of  $1920 \times 1080$   
276 pixels, 8-bit color depth and a refresh rate of 60 Hz, viewed at a distance of 70 cm. The mean  
277 luminance was  $69.93 \text{ cd/m}^2$  and contrast was 95%. The diameter of the circular aperture in  
278 which the wallpaper pattern appeared was  $13.8^\circ$  of visual angle presented against a mean lumi-  
279 nance gray background. Stimulus presentation was controlled using in-house software. For the  
280 psychophysics experiment, the stimuli were shown on a  $48 \times 27 \text{ cm}$  VIEWPiXX/3D LCD Display  
281 monitor, model VPX-VPX-2005C, resolution  $1920 \times 1080$  pixels, with a viewing distance of ap-  
282 proximately 40cm and linear gamma. Stimulus presentation was controlled using MatLab and  
283 Psychtoolbox-3 (Kleiner et al., 2007; Brainard, 1997). The diameter of the circular aperture for  
284 the stimuli was  $21.5^\circ$ .

285 **EEG Procedure**

286 Visual Evoked Potentials were measured using a steady-state design, in which  $P_1$  control images  
287 alternated with exemplar images from each of the 16 other wallpaper groups. Exemplar images  
288 were always preceded by their matched  $P_1$  control image. A single 0.83 Hz stimulus cycle consisted  
289 of a control  $P_1$  image followed by an exemplar image, each shown for 600 ms. A trial consisted  
290 of 10 such cycles (12 sec) over which 10 different exemplar images and matched controls from  
291 the same rotation group were presented. For each group type, the individual exemplar images

were always shown in the same order within the trials. Participants initiated each trial with a button-press, which allowed them to take breaks between trials. Trials from a single wallpaper group were presented in blocks of four repetitions, which were themselves repeated twice per session, and shown in random order within each session. To control fixation, the participants were instructed to fixate a small white cross in the center of display. To control vigilance, a contrast dimming task was employed. Two times per trial, an image pair was shown at reduced contrast, and the participants were instructed to press a button on a response pad. We adjusted the contrast reduction such that average accuracy for each participant was kept at 85% correct, in order to keep the difficulty of the vigilance at a constant level.

### Psychophysics Procedure

The experiment consisted of 16 blocks, one for each of the wallpaper groups (excluding  $P_1$ ). We used a two-interval forced choice approach. In each trial, participants were presented with two stimuli (one of which was the wallpaper group for the current block of trials, the other being  $P_1$ ), one after the other (inter-stimulus interval of 700ms). After each stimulus had been presented, it was masked with white noise for 300ms. After both stimuli had been presented, participants made a response on the keyboard to indicate whether they thought the first or second image contained more symmetry. Each block started with 10 practice trials, (stimulus display duration of 500ms) to allow participants to familiarise themselves with the current block's wallpaper pattern. If they achieved an accuracy of 9/10 in these trials they progressed to the rest of the block, otherwise they carried out another set of 10 practise trials. This process was repeated until the required accuracy of 9/10 was obtained. The rest of the block consisted of four interleaved staircases (using the QUEST algorithm (Watson and Pelli, 1983), full details given in the SI) of 30 trials each. On average, a block of trials took around 10 minutes to complete.

### EEG Acquisition and Preprocessing

Steady-State Visual Evoked Potentials (SSVEPs) were collected with 128-sensor HydroCell Sensor Nets (Electrical Geodesics, Eugene, OR) and were band-pass filtered from 0.3 to 50 Hz. Raw data were evaluated off line according to a sample-by-sample thresholding procedure to remove noisy sensors that were replaced by the average of the six nearest spatial neighbors. On average, less than 5% of the electrodes were substituted; these electrodes were mainly located near the forehead or the ears. The substitutions can be expected to have a negligible impact on our results, as the majority of our signal can be expected to come from electrodes over occipital, temporal and parietal cortices. After this operation, the waveforms were re-referenced to the common average of all the sensors. The data from each 12s trial were segmented into five 2.4 s long epochs (i.e., each of these epochs was exactly 2 cycles of image modulation). Epochs for which a large percentage of data samples exceeding a noise threshold (depending on the participant and ranging between 25 and 50  $\mu$ V) were excluded from the analysis on a sensor-by-sensor basis. This was typically the case for epochs containing artifacts, such as blinks or eye movements. Steady-state stimulation will drive cortical responses at specific frequencies directly tied to the stimulus frequency. It is thus appropriate to quantify these responses in terms of both phase and amplitude. Therefore, a

331 Fourier analysis was applied on every remaining epoch using a discrete Fourier transform with a  
332 rectangular window. The use of two-cycle long epochs (i.e., 2.4 s) was motivated by the need to  
333 have a relatively high resolution in the frequency domain,  $\delta f = 0.42$  Hz. For each frequency bin,  
334 the complex-valued Fourier coefficients were then averaged across all epochs within each trial.  
335 Each participant did two sessions of 8 trials per condition, which resulted in a total of 16 trials  
336 per condition.

### 337 SSVEP Analysis

338 Response waveforms were generated for each group by selective filtering in the frequency do-  
339 main. For each participant, the average Fourier coefficients from the two sessions were averaged  
340 over trials and sessions. The SSVEP paradigm we used allowed us to separate symmetry-related  
341 responses from non-specific contrast transient responses. Previous work has demonstrated that  
342 symmetry-related responses are predominantly found in the odd harmonics of the stimulus fre-  
343 quency, whereas the even harmonics consist mainly of responses unrelated to symmetry, that  
344 arise from the contrast change associated with the appearance of the second image (Norcia et al.,  
345 2002; Kohler et al., 2016). This functional distinction of the harmonics allowed us to generate  
346 a single-cycle waveform containing the response specific to symmetry, by filtering out the even  
347 harmonics in the spectral domain, and then back-transforming the remaining signal, consisting  
348 only of odd harmonics, into the time-domain. For our main analysis, we averaged the odd har-  
349 monic single-cycle waveforms within a six-electrode region of interest (ROI) over occipital cortex  
350 (electrodes 70, 74, 75, 81, 82, 83). These waveforms, averaged over participants, are shown in  
351 Figure 1. The same analysis was done for the even harmonics and for the odd harmonics within a  
352 six electrode ROI over parietal cortex (electrodes 53, 54, 61, 78, 79, 86; see Supplementary Figure  
353 1.1). The root-mean square values of these waveforms, for each individual participant, were used  
354 to determine whether each of the wallpaper subgroup relationships were preserved in the brain  
355 data.

### 356 Defining the list of subgroup relationships

357 In order to get the complete list of subgroup relationships, we digitized Table 4 from Coxeter  
358 (Coxeter and Moser, 1972) (shown in Supplementary Table 1.2). After removing identity rela-  
359 tionships (i.e. each group is a subgroup of itself) and the three pairs of wallpaper groups that are  
360 subgroups of each other (e.g. *PM* is a subgroup of *CM*, and *CM* is a subgroup of *PM*) we were left  
361 with a total of 63 unambiguous subgroups that were included in our analysis.

### 362 Bayesian Analysis of SSVEP and Psychophysical data

363 Bayesian analysis was carried out using R (v3.6.1) (R Core Team, 2019) with the *brms* package  
364 (v2.9.0) (Bürkner, 2017) and *rStan* (v2.19.2 (Stan Development Team, 2019)). The data from each  
365 experiment were modelled using a Bayesian generalised mixed effect model with wallpaper group  
366 being treated as a 16-level factor, and random effects for participant. The SSVEP data and sym-  
367 metry detection threshold durations were modelled using log-normal distributions with weakly

informative,  $\mathcal{N}(0, 2)$ , priors. After fitting the model to the data, samples were drawn from the posterior distribution of the two datasets, for each wallpaper group. These samples were then recombined to calculate the distribution of differences for each of the 63 pairs of subgroup and supergroup. These distributions were then summarised by computing the conditional probability of obtaining a positive (negative) difference,  $p(\Delta|\text{data})$ . For further technical details, please see the Supplementary Materials at <https://osf.io/f3ex8/> where the full R code, model specification, prior and posterior predictive checks, and model diagnostics, can be found.

## References

- Apthorp, D. and Bell, J. (2015). Symmetry is less than meets the eye. *Current Biology*, 25(7):R267–R268.
- Attneave, F. (1954). Some informational aspects of visual perception. *Psychol Rev*, 61(3):183–93.
- Barlow, H. B. (1961). *Possible principles underlying the transformations of sensory messages*, pages 217–234. MIT Press.
- Brainard, D. H. (1997). Spatial vision. *The psychophysics toolbox*, 10:433–436.
- Bürkner, P.-C. (2017). Advanced bayesian multilevel modeling with the r package brms. *arXiv preprint arXiv:1705.11123*.
- Clarke, A. D. F., Green, P. R., Halley, F., and Chantler, M. J. (2011). Similar symmetries: The role of wallpaper groups in perceptual texture similarity. *Symmetry*, 3(4):246–264.
- Cohen, E. H. and Zaidi, Q. (2013). Symmetry in text: Salience of mirror symmetry in natural patterns. *Journal of vision*, 13(6).
- Coxeter, H. S. M. and Moser, W. O. J. (1972). *Generators and relations for discrete groups*. Ergebnisse der Mathematik und ihrer Grenzgebiete ; Bd. 14. Springer-Verlag, Berlin, New York.
- Fedorov, E. (1891). Symmetry in the plane. In *Zapiski Imperatorskogo S. Peterburgskogo Mineralogicheskogo Obshchestva [Proc. S. Peterb. Mineral. Soc.]*, volume 43, pages 345–390.
- Field, D. J. (1987). Relations between the statistics of natural images and the response properties of cortical cells. *J Opt Soc Am A*, 4(12):2379–94.
- Geisler, W. S., Najemnik, J., and Ing, A. D. (2009). Optimal stimulus encoders for natural tasks. *Journal of Vision*, 9(13):17–17.
- Hoyle, R. B. (2006). *Pattern formation: an introduction to methods*. Cambridge University Press.
- Jablan, S. V. (2014). *Symmetry, Ornament and Modularity*. World Scientific Publishing Co Pte Ltd, Singapore, SINGAPORE.
- Keefe, B. D., Gouws, A. D., Sheldon, A. A., Vernon, R. J. W., Lawrence, S. J. D., McKeefry, D. J., Wade, A. R., and Morland, A. B. (2018). Emergence of symmetry selectivity in the visual areas of the human brain: fMRI responses to symmetry presented in both frontoparallel and slanted planes. *Human Brain Mapping*, 39(10):3813–3826.
- Kleiner, M., Brainard, D., Pelli, D., Ingling, A., Murray, R., and Broussard, C. (2007). What's new in psychtoolbox-3. *Perception*, 36:1–16.
- Kohler, P. J., Clarke, A., Yakovleva, A., Liu, Y., and Norcia, A. M. (2016). Representation of maximally regular textures in human visual cortex. *The Journal of Neuroscience*, 36(3):714–729.
- Kohler, P. J., Cottereau, B. R., and Norcia, A. M. (2018). Dynamics of perceptual decisions about symmetry in visual cortex. *NeuroImage*, 167(Supplement C):316–330.
- Landwehr, K. (2009). Camouflaged symmetry. *Perception*, 38:1712–1720.
- Laughlin, S. (1981). A simple coding procedure enhances a neuron's information capacity. *Z Naturforsch C*, 36(9-10):910–2.
- Leopold, D. A., Bondar, I. V., and Giese, M. A. (2006). Norm-based face encoding by single neu-

- 439 rons in the monkey inferotemporal cortex. *Nature*,  
440 442(7102):572–5.
- 441 Li, Y., Sawada, T., Shi, Y., Steinman, R., and Pizlo, Z.  
442 (2013). *Symmetry Is the sine qua non of Shape*, book section 2, pages 21–40. Advances in Computer Vision  
443 and Pattern Recognition. Springer London.
- 444
- 445 Liu, Y., Hel-Or, H., Kaplan, C. S., and Van Gool,  
446 L. (2010). Computational symmetry in computer  
447 vision and computer graphics. *Foundations and  
448 Trends® in Computer Graphics and Vision*, 5(1–2):1–  
449 195.
- 450 Liu, Y., Lin, W.-C., and Hays, J. (2004). Near-regular  
451 texture analysis and manipulation. In *ACM Trans-  
452 actions on Graphics (TOG)*, volume 23, pages 368–  
453 376. ACM.
- 454 Makin, A. D. J., Wright, D., Rampone, G., Palumbo,  
455 L., Guest, M., Sheehan, R., Cleaver, H., and  
456 Bertamini, M. (2016). An Electrophysiological  
457 Index of Perceptual Goodness. *Cerebral Cortex*,  
458 26(12):4416–4434.
- 459 Møller, A. P. (1992). Female swallow preference  
460 for symmetrical male sexual ornaments. *Nature*,  
461 357(6375):238–240.
- 462 Norcia, A. M., Appelbaum, L. G., Ales, J. M., Co  
463 tereau, B. R., and Rossion, B. (2015). The steady  
464 state visual evoked potential in vision research:  
465 review. *Journal of Vision*, 15(6):4–4.
- 466 Norcia, A. M., Candy, T. R., Pettet, M. W., Vildavski,  
467 V. Y., and Tyler, C. W. (2002). Temporal dyna  
468 mics of the human response to symmetry. *Journal of  
469 Vision*, 2(2):132–139.
- 470 Nucci, M. and Wagemans, J. (2007). Goodness of  
471 Regularity in Dot Patterns: Global Symmetry, Lo  
472 cal Symmetry, and Their Interactions. *Perception*,  
473 36(9):1305–1319. Publisher: SAGE Publications  
474 Ltd STM.
- 475 Olshausen, B. A. and Field, D. J. (1997). Sparse cod  
476 ing with an overcomplete basis set: a strategy em  
477 ployed by v1? *Vision Res*, 37(23):3311–25.
- 479 Palmer, S. E. (1985). The role of symmetry in shape  
perception. *Acta Psychologica*, 59(1):67–90.
- 480 Polya, G. (1924). Xii. Über die analogie der  
kristallsymmetrie in der ebene. *Zeitschrift für  
Kristallographie-Crystalline Materials*, 60(1):278–282.
- 481
- 482 R Core Team (2019). *R: A Language and Environment  
for Statistical Computing*. R Foundation for Statistical  
483 Computing, Vienna, Austria.
- 484 Ramachandran, V. S. and Hirstein, W. (1999). The  
science of art: A neurological theory of aesthetic  
experience. *Journal of Consciousness Studies*, 6(6–  
7):15–41.
- 485 Sasaki, Y., Vanduffel, W., Knutson, T., Tyler, C., and  
Tootell, R. (2005). Symmetry activates extrastriate  
visual cortex in human and nonhuman primates.  
*Proceedings of the National Academy of Sciences of the  
United States of America*, 102(8):3159–3163.
- 486 Stan Development Team (2019). RStan: the R inter  
face to Stan. R package version 2.19.2.
- 487 Tinbergen, N. (1953). *The herring gull's world: a study  
of the social behaviour of birds*. Frederick A. Praeger,  
Inc., Oxford, England.
- 488 van der Helm, P. A. and Leeuwenberg, E. L. J. (1996).  
Goodness of visual regularities: A nontransformational  
approach. *Psychological Review*, 103(3):429–  
456. Publisher: American Psychological Association.
- 489
- 490 Wagemans, J., Van Gool, L., and d'Ydewalle, G.  
491 (1991). Detection of symmetry in tachistoscopically  
492 presented dot patterns: effects of multiple axes and  
skewing. *Perception & Psychophysics*,  
493 50(5):413–27.
- 494 Watson, A. B. and Pelli, D. G. (1983). Quest: A  
bayesian adaptive psychometric method. *Percep  
495 tion & Psychophysics*, 33(2):113–120.
- 496 Webster, M. A. and MacLin, O. H. (1999). Figural  
497 aftereffects in the perception of faces. *Psychon Bull  
498 Rev*, 6(4):647–53.